

Kinetics of Disassembly of a DNA-Bound Porphyrin Supramolecular Array

Robert F. Pasternack,^{*,†} Esther J. Gibbs,[‡] Derek Bruzewicz,[†] David Stewart,[†] and Kelly Shannon Engstrom[†]

Contribution from the Department of Chemistry, Swarthmore College, Swarthmore, Pennsylvania 19081, and the Department of Chemistry, Goucher College, Towson, Maryland 21204

Received November 6, 2001

Abstract: *trans*-Bis(*N*-methylpyridinium-4-yl)diphenylporphine forms extended, organized assemblies on DNA templates under appropriate conditions of concentration, ionic strength, and temperature. Addition of β -cyclodextrin to these arrays leads to their disassembly as evidenced by changes in extinction, circular dichroism, and resonance light scattering spectra. The structure or flexibility of the polymer template has an effect on the rate of disassembly; the reaction is faster on a poly(dG-dC)₂ surface than on ct DNA. The kinetic profiles for the disassembly process can be fit with great precision with a two-kinetic parameter equation in which the rate constant is itself a function of time. The reaction rate, studied in the presence of excess β -CD, shows a dependence on the *mode of detection*. A model is presented to account for these observations in which the arrays become increasingly reactive with time due to β -CD attack at the interior of the porphyrin assemblies as well as the ends.

Introduction

Descriptions of the interactions of cationic porphyrins and metalloporphyrins with DNA have been reported in several review articles, and although differences in emphasis are apparent in these summaries, they have a number of basic features in common.^{1–3} General agreement exists that some porphyrin derivatives are capable of intercalating into DNAs of appropriate composition, while other porphyrins—as a result of the nature of peripheral substituents or inserted metal—are limited to external, groove binding. In addition, evidence has been presented for porphyrin self-assembly on a DNA surface.^{4–8} In some instances, these aggregates are relatively modest in size,^{4,5} but for at least two derivatives, compelling evidence has been presented for highly extended assemblies.^{6–8} The free base and copper(II) derivatives of *trans*-bis(*N*-methylpyridinium-4-yl)diphenylporphine (*t*-H₂P_{agg}; Figure 1) and a “tentacle” porphyrin each provide spectroscopic signatures consistent with

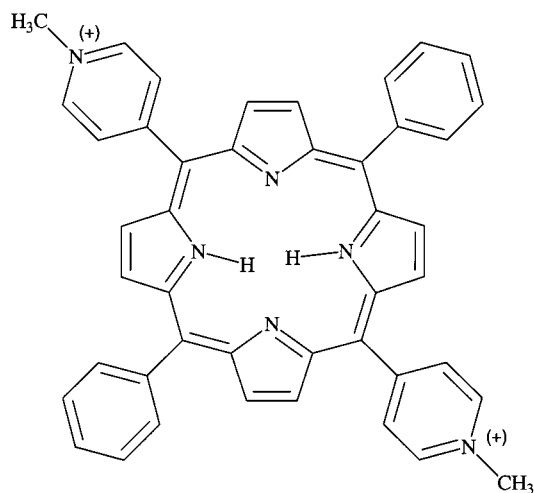


Figure 1. Structure of the free base porphyrin *trans*-bis(*N*-methylpyridinium-4-yl)diphenylporphine (*t*-H₂P_{agg}).

the formation of extended, electronically coupled, organized assemblies on DNA. Particularly useful for identifying and characterizing these aggregates have been circular dichroism (CD)⁷ and the newly developed resonance light scattering (RLS) method.⁹ Through a combination of extinction spectroscopy, circular dichroism, and resonance light scattering, it has been shown that the assemblies can reach very large sizes, in excess of 10⁵ molecules/array unit.^{10,11} Beyond some threshold drug load, called the critical assembly concentration or cac, all added

* To whom correspondence should be addressed. E-mail: rpaster1@swarthmore.edu.

[†] Swarthmore College.

[‡] Goucher College.

- (1) Pasternack, R. F.; Gibbs, E. J. In *Probing of Nucleic Acids by Metal Complexes of Small Molecules*; Sigel, A., Sigel, H., Eds.; Metal Ions in Biological Systems 33; Marcel Dekker: New York, 1996; pp 367–397.
- (2) Fiel, R. J. *J. Biomol. Struct. Dyn.* **1989**, *6*, 1259–1274.
- (3) Marzilli, L. G. *New J. Chem.* **1990**, *14*, 409–420.
- (4) Carvlin, M. J.; Datta-Gupta, N.; Fiel, R. J. *Biochem. Biophys. Res. Commun.* **1982**, *108*, 66–73.
- (5) Pasternack, R. F.; Gibbs, E. J.; Villafranca, J. J. *Biochemistry* **1983**, *22*, 2406–2414.
- (6) Gibbs, E. J.; Tinoco, I., Jr.; Maestre, M. F.; Ellinas, P. A.; Pasternack, R. F. *Biochim. Biophys. Res. Commun.* **1988**, *157*, 350–358.
- (7) Pasternack, R. F.; Giannetto, A.; Pagano, P.; Gibbs, E. J. *J. Am. Chem. Soc.* **1991**, *113*, 7799–7800.
- (8) Marzilli, L. G.; Petho, G.; Lin, M.; Kim, M. S.; Dixon, D. W. *J. Am. Chem. Soc.* **1992**, *114*, 7575–7577.

- (9) Pasternack, R. F.; Bustamante, C.; Collings, P. J.; Giannetto, A.; Gibbs, E. J. *J. Am. Chem. Soc.* **1993**, *115*, 5393–5399.
- (10) Collings, P. J.; Gibbs, E. J.; Starr, T. E.; Vafek, O.; Yee, C.; Pomerance, L. A.; Pasternack, R. F. *J. Phys. Chem. B* **1999**, *103*, 8474–8481.

porphyrin becomes part of *aggregates*; the critical concentration of monomer at equilibrium depends on both ionic strength and temperature.¹²

Kinetics of aggregate formation have been investigated for both $t\text{-H}_2\text{P}_{\text{agg}}$ and $t\text{-CuP}_{\text{agg}}$ on DNA.^{11,13} The time-dependent profiles obtained for the porphyrin-assembly process generally begin with an induction phase, followed by a period of rapid growth, and then by a gradual approach to equilibrium. A nonconventional autocatalytic mechanism was proposed for the aggregation in which the growing assembly catalyzes the formation of new reaction centers for polymerization.¹³ The formation of these reaction centers (referred to also as “nuclei” or “seeds”) is putatively the rate-determining step in the overall aggregation process. As implied by the term “autocatalysis”, the system becomes increasingly reactive with time, which manifests itself in this analysis in time-dependent rate constants.

The proposed rate law, written to reflect the reversibility of the process and the unusual form of the mass action expression (i.e., $K = \text{cac} = [\text{M}_i]$), is given by the equation

$$-d[\text{M}]/dt = k(t)\{([\text{M}] - [\text{M}_i])^m/([\text{M}_0] - [\text{M}_i])^{m-1}\} \quad (1)$$

where m is related to the number of molecules that comprise the reaction nucleus, $[\text{M}]$ is the concentration of monomer at time t , $[\text{M}_0]$ is the initial concentration of porphyrin, and $[\text{M}_i]$ is the concentration of monomer at equilibrium. The form of the rate constant, $k(t)$, is considered next. In the absence of a catalyst, the reaction proceeds with a time-independent rate constant, k_0 . However, as a consequence of autocatalysis, a second term is included that is *time-dependent*. Using the model of surface-catalyzed reactions as a guide, the catalytic rate constant is expected to be proportional to the *aggregate size*. For fractal aggregates, cluster size has been shown to increase with a power-law dependence on time,¹⁴ and therefore, it has been proposed that the overall rate constant, $k(t)$, can be written as¹³

$$k(t) = k_0 + k_c(k_c t)^n \quad (2)$$

where the parameter n is related to the growth rate of the aggregate. The differential rate law (eq 1) is integrated to give

$$[\text{M}] = [\text{M}_i] + ([\text{M}_0] - [\text{M}_i])\left\{(1 + (m-1)k_0 t + (n+1)^{-1}(k_c t)^{n+1})^{-1/(m-1)}\right\} \quad (3)$$

for $m \neq 1$.

This nonconventional approach has been used with some considerable success for the investigation of assembly formation of $t\text{-H}_2\text{P}_{\text{agg}}$ and $t\text{-CuP}_{\text{agg}}$ on DNA.^{11,13,15} In addition, the model proves capable of fitting literature data for several biologically important assembly processes, including actin polymerization and the formation of β -amyloid aggregates.^{11,13,16} Fuller ap-

plicability and the implications of this kinetic model are now under active investigation.

In the present paper, we consider an equally important, but heretofore largely unexplored area of supramolecular chemistry. We describe studies on the kinetics of *assembly degradation*. These experiments are begun with a fully formed, equilibrated array of DNA-bound porphyrins. Then, through the addition of β -CD, the DNA surface is cleared of porphyrin ligands with the formation of $t\text{-H}_2\text{P}_{\text{agg}}/\beta\text{-CD}$ complexes. We report here on the nature of the porphyrin product and the mechanistic implications of the degradation kinetics.

Experimental Section

Materials. The porphyrin used for this study, *trans*-bis(*N*-methylpyridinium-4-yl)diphenylporphine (Figure 1) was prepared from *trans*-bis(pyridinium-4-yl)diphenylporphine supplied by Mid-Century Chemicals (Chicago, IL). The starting material (75 mg) was refluxed for 48 h in 150 mL of a 1:1 mixture of iodomethane and methylene chloride. The product, after evaporation of the solvent system, was treated with a Dowex anion-exchange resin to convert the iodide salt to the more soluble chloride form. The ¹H NMR spectrum of the final product was identical to that obtained with a fully characterized authentic sample. Stock solutions, prepared from the solid in purified filtered water, were stored in the dark. Porphyrin concentrations were determined in 1 mM phosphate buffer, pH ~7, using a value for the molar absorptivity of $\epsilon = 2.40 \times 10^5 \text{ M}^{-1} \text{ cm}^{-1}$ at the Soret maximum near 419 nm.¹⁷ Both poly(dG-dC)₂ and calf thymus DNA were obtained from Pharmacia Biotech (Piscataway, NJ). The former polynucleotide was purified by extensive dialysis against a solution consisting of 1 mM phosphate buffer and 8 mM NaCl. Calf thymus DNA was purified using a standard method described previously.⁵ Concentrations, expressed in moles of base pairs per liter, were obtained using $\epsilon = 1.48 \times 10^4 \text{ M}^{-1} \text{ cm}^{-1}$ for poly(dG-dC)₂¹⁸ and $\epsilon = 1.32 \times 10^4 \text{ M}^{-1} \text{ cm}^{-1}$ for ct DNA,¹⁹ both at the UV maximums near 260 nm. The integrity of the double helix was monitored via circular dichroism.

Both α - and γ -cyclodextrins were purchased from Sigma-Aldrich Co. and used without further purification. Sigma-Aldrich also supplied the β -cyclodextrin (β -CD) used in this study, but this product was twice recrystallized from warm water. All other chemicals, obtained from Fisher Scientific, were reagent grade and used without additional purification. Water, purified through a Barnstead Nanopure water system, was passed through 0.2- μm Nalgene syringe filters immediately prior to use in solution preparation. All stock solutions, except those containing nucleic acids, were also filtered.

Methods. Absorbance (extinction) measurements were conducted on a Jasco V550 spectrophotometer using Fisher methacrylate cuvettes whenever possible. The temperature was maintained at $24.5 \pm 0.1^\circ$. Porphyrin staining of the cuvette surfaces is less severe for methacrylate than quartz cuvettes, and so the latter cuvettes were reserved for experiments conducted in the ultraviolet region and for circular dichroism experiments performed on an Aviv 62DS spectrometer. Fluorescence and RLS measurements were conducted on a SPEX Fluorolog spectrofluorometer. The RLS method, as previously described,^{9,20} uses a “synchronous scan” mode in which the emission and excitation monochromators are preset to identical wavelengths.

Solutions of DNA-bound porphyrin assemblies were prepared using a protocol in which the porphyrin was added to DNA in 1 mM phosphate buffer, pH ~7; NaCl was added last. We showed previously⁷ that reproducible results for the assembly process are obtained when

(11) Pasternack, R. F.; Ewen, S.; Rao, A.; Meyer, A. S.; Freedman, M. A. *Inorg. Chim. Acta* **2001**, *317*, 59–71.

(12) Pasternack, R. F.; Goldsmith, J. I.; Szep, S.; Gibbs, E. J. *Biophys. J.* **1998**, *75*, 1024–1031.

(13) Pasternack, R. F.; Gibbs, E. J.; Collings, P. J.; de Paula, J. C.; Turzo, L. C.; Terracina, A. *J. Am. Chem. Soc.* **1998**, *120*, 5873–5878.

(14) Leyvraz, F. In *On Growth and Form*; Stanley, H. E., Ostrowsky, N., Eds.; Martinus Nijhoff Publishers: Dordrecht, 1986; pp 136–144.

(15) Freedman, M.; Pasternack, R. F. *Chemist* **2000**, *77*, 25–31.

(16) Pasternack, R. F.; Fleming, C.; Herring, S.; Collings, P. J.; de Paula, J.; DeCastro, G.; Gibbs, E. J. *Biophys. J.* **2000**, *79*, 550–560.

(17) Sari, M. A.; Battioni, J. P.; Dupre, D.; Mansuy, D.; Le Pecq, J. B. *Biochemistry* **1990**, *29*, 4205–4215.

(18) Wells, R. D.; Larson, J. E.; Grant, R. C.; Shortle, B. E.; Cantor, C. R. *J. Mol. Biol.* **1970**, *54*, 465–497.

(19) Pachter, J. A.; Huang, C. H.; Duvernay, V. H.; Prestayko, A. W.; Crooke, S. T. *Biochemistry* **1982**, *21*, 1541–1547.

(20) Pasternack, R. F.; Collings, P. J. *Science* **1995**, *269*, 935–939.

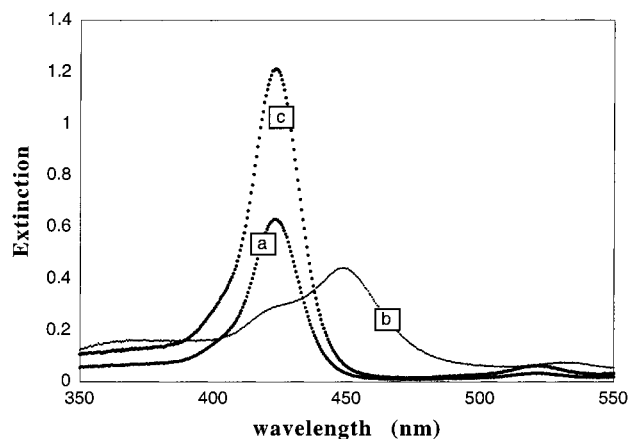


Figure 2. Extinction spectra of $t\text{-H}_2\text{P}_{\text{agg}}/\text{ct DNA}$ solutions, 1.0 mM phosphate buffer (pH ~ 7), at various conditions: (a) 8.0 mM NaCl; (b) 0.10 M NaCl; (c) equilibrated in 0.10 M NaCl followed by the addition of $\beta\text{-CD}$ to 5.0 mM.

the porphyrin, in its monomeric form, is permitted to interact with the nucleic acid prior to the addition of salt to induce aggregation.

Due to the speed of the deaggregation reaction, kinetic scans limited by hand-mixing of the reactant solutions miss a significant portion of the signal change. An RX-1000 rapid mixer (Photophysics) was employed to monitor the kinetics. The instrument incorporates a blackened quartz cuvette (having small transparent windows on all four sides) attached to driving syringes via an umbilical cord through which the unmixed solutions travel to the cell. The windows are located low on the cuvette, and fabricated risers were employed to allow for various beam heights of instruments. The temperature was maintained at 24.5 ± 0.2 °C. For each kinetics experiment, one syringe contained 1 mM phosphate buffer, 0.10 M NaCl, and double the target concentration of both $t\text{-H}_2\text{P}_{\text{agg}}$ and DNA; the other syringe contained the same phosphate and NaCl concentrations, but no porphyrin or DNA and twice the target $\beta\text{-cyclodextrin}$ concentration. “Blank” experiments were performed by mixing aggregate samples with a buffer and salt solution without $\beta\text{-CD}$ to examine dilution effects.

Extinction and circular dichroism measurements were conducted at 450 nm whereas resonance light scattering kinetics runs were performed at 535 nm for poly(dG-dC)₂ and at 570 nm for ct DNA. These latter wavelengths correspond to Q-bands of the aggregate where the absorbance is low at the concentrations used in these experiments, thus circumventing the need for absorption corrections.

Results

The manner in which $t\text{-H}_2\text{P}_{\text{agg}}$ interacts with DNA depends sensitively upon concentration, nucleic acid composition, temperature, and solvent conditions. For example, at a porphyrin concentration of 5 μM , ct DNA at 25 μM , 1 mM phosphate buffer (pH ~ 7), and 8 mM NaCl, the porphyrin remains almost totally monomeric on the nucleic acid template at 24.5 °C. The Soret region is characterized by a single peak at 422 nm (Figure 2a), and it is only through the application of more sensitive spectroscopic techniques—circular dichroism and especially resonance light scattering—that evidence can be found for the presence of any porphyrin aggregate. The Soret maximum has undergone a bathochromic shift of ~ 5 nm, with some 50% hypochromicity relative to the porphyrin free in solution under these ionic strength and pH conditions. Addition of 0.10 M NaCl has a profound effect on the solution species stable at equilibrium, as evidenced by dramatic changes in extinction (preferred to absorption because of the scattering contribution), circular dichroism, and RLS spectra. As previously described, a peak

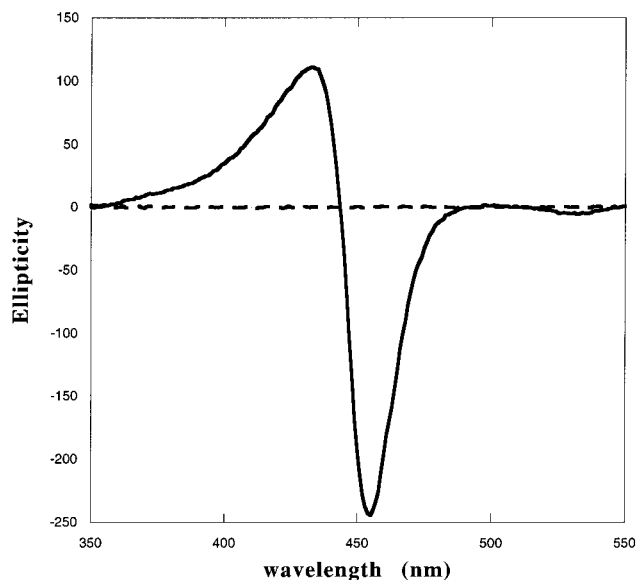


Figure 3. Circular dichroism spectra of $t\text{-H}_2\text{P}_{\text{agg}}/\text{poly}(\text{dG-dC})_2$ solutions, 1.0 mM phosphate solution, 0.10 M NaCl, no $\beta\text{-CD}$ added (—); after addition of 4.0 mM $\beta\text{-CD}$ (- - -).

of Soret intensity is observed near 450 nm (Figure 2b), the circular dichroism signal in this region is very large and bisignate, and a markedly enhanced RLS signal is observed. We have identified these spectral changes as resulting from the formation of extended organized assemblies of the porphyrin molecular ions on the DNA template.⁹ When the solution of Figure 2b is made 5 mM in $\beta\text{-cyclodextrin}$, spectrum 2c is obtained having a maximum at 423 nm. In addition, the enhanced RLS and circular dichroism signals disappear and the quantum yield for fluorescence increases. Similar results are obtained for poly(dG-dC)₂ as template, as shown in Figure 3. The enormous, bisignate circular dichroism signal of the organized porphyrin array disappears in the presence of excess $\beta\text{-CD}$. The $\beta\text{-CD}$ has apparently reversed the assembly process by forming a complex with $t\text{-H}_2\text{P}_{\text{agg}}$. Neither $\alpha\text{-CD}$ nor $\gamma\text{-CD}$ is capable of competing with the porphyrin/porphyrin interactions involved in array formation, and thus, these two cyclodextrins have little impact on the extinction, circular dichroism, or RLS spectra of assembled $t\text{-H}_2\text{P}_{\text{agg}}$.

To achieve a fuller understanding of the $t\text{-H}_2\text{P}_{\text{agg}}/\beta\text{-CD}$ interaction, both spectrophotometric and spectrofluorometric titrations of the free base porphyrin under *nonaggregating conditions* were carried out. Close examination of the titration spectra reveals that there is no persistent isosbestic point in the course of the titration (Figure 4). The data were analyzed for stepwise equilibria allowing for three chromophores, the uncomplexed porphyrin, a 1:1 complex, and a 1:2 complex (porphyrin- $\beta\text{-CD}$). An equation of the form

$$A = [t\text{-H}_2\text{P}_{\text{agg}}]_0 (\epsilon_0 + \epsilon_1 K_1 [\beta\text{-CD}]_0 + \epsilon_2 K_1 K_2 [\beta\text{-CD}]_0^2) / (1 + K_1 [\beta\text{-CD}]_0 + K_1 K_2 [\beta\text{-CD}]_0^2) \quad (4)$$

was used for these equilibria, in which A is the absorbance at a given wavelength; ϵ_0 , ϵ_1 , and ϵ_2 are the molar absorptivities of the uncomplexed, 1:1 complex and 1:2 complex, respectively; and K_1 and K_2 are the association equilibrium constants. A plot of the data at 417 nm (near the Soret maximum of the porphyrin monomer in aqueous solution) and the fit provided by eq 4 is

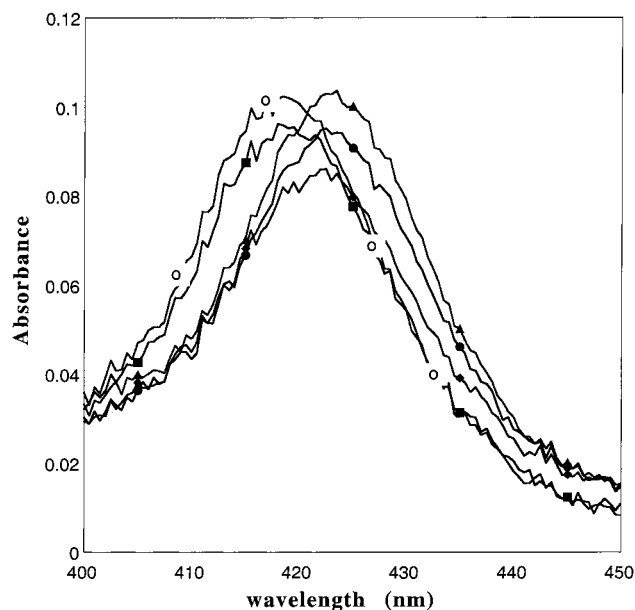


Figure 4. Titration of $0.40 \mu\text{M}$ $t\text{-H}_2\text{P}_{\text{agg}}$ with $\beta\text{-CD}$ in 1.0 mM phosphate buffer and 8.0 mM NaCl. These conditions were selected to avoid porphyrin aggregation. (O), no $\beta\text{-CD}$ added, (■) $1.8 \mu\text{M}$ $\beta\text{-CD}$, and (◆) 0.50 , (●) 2.5 , and (▲) 5.0 mM $\beta\text{-CD}$.

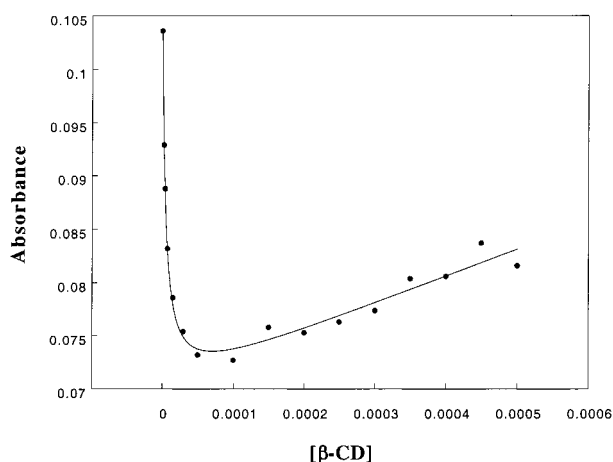


Figure 5. Absorbance titration data at 417 nm vs $[\beta\text{-CD}]$. The smooth curve shown in the figure was generated using eq 4.

shown in Figure 5. We obtain $K_1 = 2.2 \times 10^5 \text{ M}^{-1}$, $K_2 \sim 100 \text{ M}^{-1}$, and $\epsilon \times 10^{-5} = 2.1, 1.4,$ and $\sim 8 \text{ M}^{-1} \text{ cm}^{-1}$, respectively. Therefore, under the conditions of the kinetic experiments to be described below, mixtures of the 1:1 and 1:2 complexes form as products.

Kinetic data for the disassembly process were obtained using several detection methods; extinction, circular dichroism, and resonance light scattering. The reactions are so rapid that ordinary hand-mixing of the reagents leads to a loss of data in the critical early stages of the reaction. Therefore, a rapid-mixing method was required for which a Photophysics RX-1000 rapid-mixing device described in the Experimental Section was used. Shown in Figure 6 are data obtained for one such kinetic experiment using the RX-1000. A solution (which had been allowed to equilibrate) containing $4.0 \mu\text{M}$ porphyrin, $25 \mu\text{M}$ poly(dG-dC)₂, 1 mM phosphate buffer, and 0.10 M NaCl was mixed with an equal volume of a solution containing 8.0 mM $\beta\text{-CD}$, in 1 mM phosphate buffer and 0.10 M NaCl. When a sample of the porphyrin/DNA solution was mixed with an equal

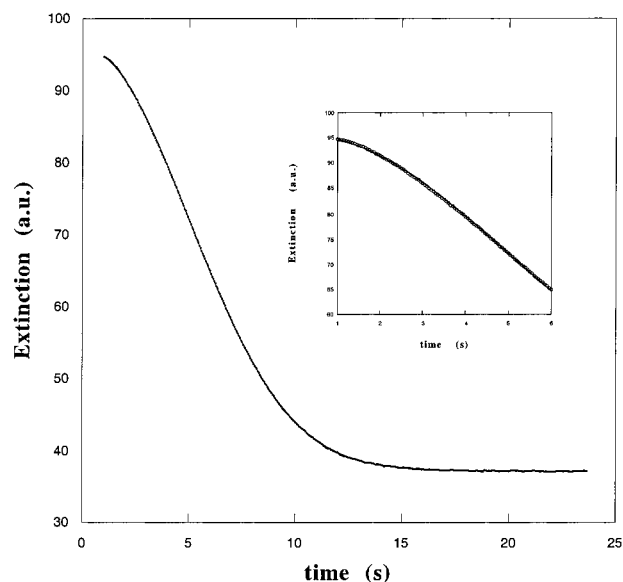


Figure 6. Kinetic study of the disassembly of a DNA-bound $t\text{-H}_2\text{P}_{\text{agg}}$ array by $\beta\text{-CD}$ at 450 nm . Conditions are $2.0 \mu\text{M}$ $t\text{-H}_2\text{P}_{\text{agg}}$, $12.5 \mu\text{M}$ poly(dG-dC)₂, 1.0 mM phosphate buffer (pH ~ 7), 0.10 M NaCl, and 4.0 mM $\beta\text{-CD}$. The curve through the points was generated using eq 5. The values obtained for k_f and n are 0.21 s^{-1} and 1.0 , respectively. (Inset) Closeup view of the early data and the fit provided by eq 5.

volume of a buffer/salt solution containing no $\beta\text{-CD}$ (dilution experiment), a very small, slow effect was observed, which could be fit as a single first-order process having a $k \sim 0.001 \text{ s}^{-1}$ for poly(dG-dC)₂ and $\sim 0.005 \text{ s}^{-1}$ for ct DNA. However, the color change is so small for these dilution experiments as to introduce considerable uncertainty as to the uniqueness of this functional form to fit the data and the value of the rate constant. In contrast, as shown in Figure 6, the addition of $\beta\text{-CD}$ leads to a large, easily detected extinction change at 450 nm . The kinetic profile could not be fit with simple, standard forms, i.e., coupled first-order, second-order, etc. Rather, the inflection in the data suggested to us that we consider an autocatalytic pathway in which rate constants can show a time dependence. In analogy to previous work on assembly formation, we considered $k(t) = k_f(k_f t)^n$, which provides a rate constant having units of reciprocal time regardless of the value of n . The smooth curve through the data, shown in the figure, was obtained using the integrated rate law:

$$E = E_{\text{inf}} + (E_0 - E_{\text{inf}}) \exp(-(k_f t)^{n+1}/(n+1)) \quad (5)$$

in which E , E_0 , and E_{inf} are the extinctions at time t , initially and at equilibrium. Note that if $n = 0$, the equation takes on the conventional first-order form, but for the data shown in Figure 6, the excellent fit was achieved with $n = 1.0$. Shown in the figure as an inset is the fit of the data for the early portion of the kinetic profile, a region that is particularly challenging for (i.e., unsatisfactorily modeled by) more standard functional forms.

The dependence of reaction rate on initial conditions of porphyrin, DNA, and $\beta\text{-CD}$ concentration was investigated. Results obtained from these experiments with poly(dG-dC)₂ are shown in Figure 7. We also investigated whether the measured reaction rate shows a dependence on detection mode, as a possible source of mechanistic information on the deaggregation process(es). For these studies, we determined values of k_f as a

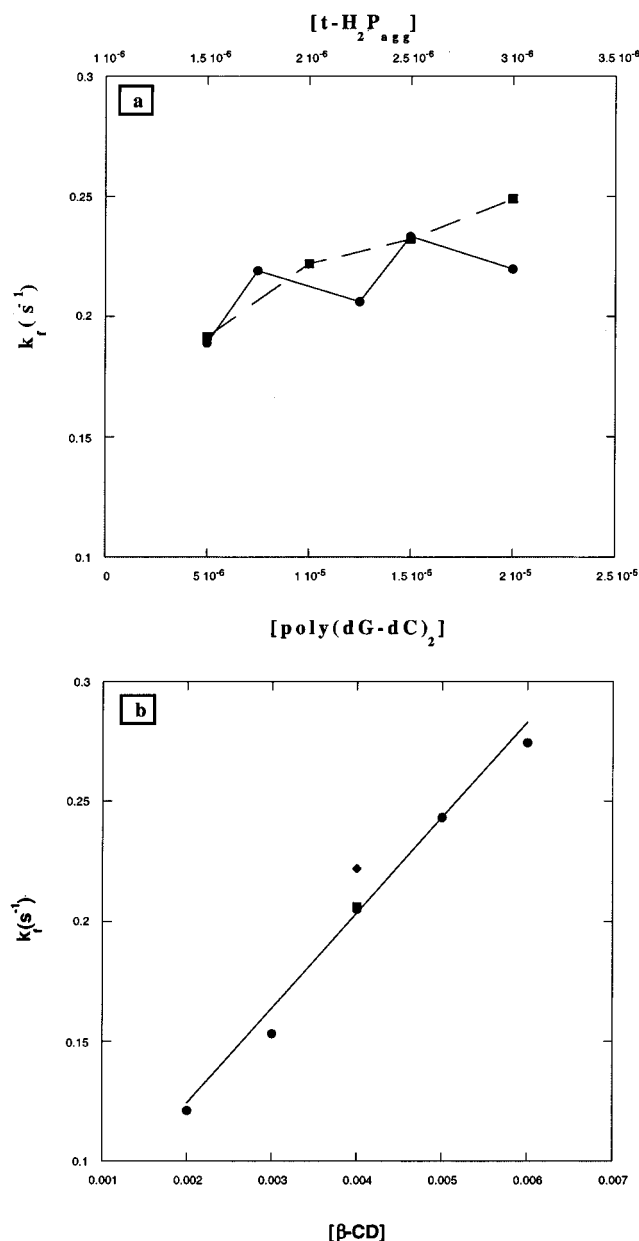


Figure 7. Dependence of the rate constant, k_f , on initial concentrations using extinction detection: (a) (---) $t\text{-H}_2\text{P}_{\text{agg}}$ and (—) $\text{poly}(\text{dG-dC})_2$; (b) $\beta\text{-CD}$. The equation for the linear plot in part b is $k_f = 0.045 + 40[\beta\text{-CD}]$ at 2.0 μM $t\text{-H}_2\text{P}_{\text{agg}}$, 12.5 μM $\text{poly}(\text{dG-dC})_2$, 1.0 mM phosphate buffer, and 0.10 M NaCl. Three separate data points are shown for 4.0 mM $\beta\text{-CD}$; these conditions were repeated several times to test the reproducibility of these kinetic results.

function of $\beta\text{-CD}$ concentration at (i) 2.0 μM $t\text{-H}_2\text{P}_{\text{agg}}$, 12.5 μM $\text{poly}(\text{dG-dC})_2$, 1 mM phosphate buffer, 0.10 M NaCl, 24.5 °C, and at (ii) 2.5 μM porphyrin, 25 μM ct DNA at the same buffer, salt, and temperature. All of extinction, circular dichroism, and RLS detection were used. For the RLS measurements, the reaction was followed at 535 or 570 nm (Q-bands of the aggregates, see Experimental Section) to avoid the necessity of absorption corrections^{10,11} that are difficult to make since they too are time-dependent. The results of these studies for $\text{poly}(\text{dG-dC})_2$ are shown in Figure 8; the rate constant dependence on $\beta\text{-CD}$ is clearly sensitive to the method of detection. Little difference is observed between RLS and circular dichroism, but the slope of the extinction versus $\beta\text{-CD}$ line is smaller (77 and

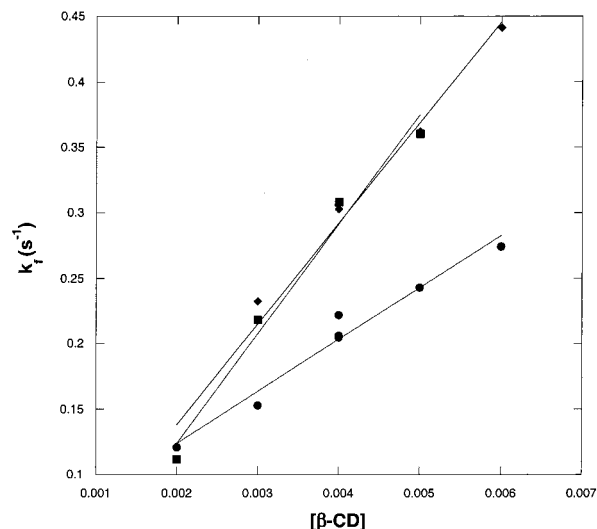


Figure 8. Dependence of k_f on $[\beta\text{-CD}]$ obtained from experiments using various detection methods: (●) extinction detection; (◆) RLS; (■) circular dichroism. The RLS and circular dichroism results have nearly identical dependences on $[\beta\text{-CD}]$; the slopes are 77 $\text{M}^{-1} \text{s}^{-1}$ for the former and 84 $\text{M}^{-1} \text{s}^{-1}$ for the latter method, whereas the slope obtained for extinction detection under the same conditions is 40 $\text{M}^{-1} \text{s}^{-1}$.

84 vs 40 $\text{M}^{-1} \text{s}^{-1}$). Similar results were obtained for ct DNA, for which the slopes are 28 and 26 $\text{M}^{-1} \text{s}^{-1}$ for RLS and circular dichroism, respectively, while the slope obtained for extinction detection under the same conditions is 16 $\text{M}^{-1} \text{s}^{-1}$. The values indicate that the more stable, rigid polynucleotide, which promotes assembly formation,^{11,15} also facilitates its degradation by $\beta\text{-CD}$.

Discussion

None of the cyclodextrin derivatives tested proved capable of removing intercalated/groove-bound $t\text{-H}_2\text{P}_{\text{agg}}$ from DNA under conditions of low drug load and ionic strength. At higher ionic strengths, the primary interaction type of the porphyrin changes to a DNA-bound supramolecular assembly, and under these conditions, $\beta\text{-cyclodextrin}$ induces deaggregation with the formation of $t\text{-H}_2\text{P}_{\text{agg}}/\beta\text{-CD}$ complexes. Neither $\alpha\text{-}$ nor $\gamma\text{-CD}$ is effective at promoting the disassembly process. Such discrimination of guests among cyclodextrin hosts is not uncommon and usually reflects differences in size and hydrophobicity of the cyclodextrin core. For example, an anionic water-soluble porphyrin, *meso*-tetra(4-sulfonatophenyl)porphine (H_2TPPS_4), has been reported to bind to cyclodextrins with order of preference $\beta\text{-CD} > \gamma\text{-CD} > \alpha\text{-CD}$.²¹

The failure of the cyclodextrins to remove porphyrins from DNA at low ionic strength is the consequence of a thermodynamic, not a kinetic barrier. If the $t\text{-H}_2\text{P}_{\text{agg}}/\beta\text{-CD}$ complex is challenged with DNA under these conditions, complete transfer to the polynucleotide is observed based upon absorbance and circular dichroism evidence. The free energy of binding of porphyrins (and other cationic drugs) to DNA is dependent on both charge type and concentration of electrolyte cations, with K_A (the association constant) decreasing with increasing electrolyte concentration.^{22,23} The porphyrin/cyclodextrin interaction is far less sensitive to ionic strength, and so the ability of

(21) Ribo, J. M.; Farrera, J.-A.; Valero, M. L.; Virgili, A. *Tetrahedron* **1995**, *51*, 3705–3712. Hamai, S.; Koshiyano, T. *J. Photochem. Photobiol. A: Chem.* **1999**, *127*, 135–141.

β -cyclodextrin to clear the DNA surface of porphyrin at high but not low NaCl concentration is not completely unanticipated. The product, at the β -CD concentrations used for the present experiments (2–8 mM), is a mixture of 1:1 and 1:2 t -H₂P_{agg}/ β -CD complexes. It should be noted that the kinetic analyses (Figures 7 and 8) lead to a linear dependence of rate constant on $[\beta$ -CD]. Therefore, the rate-determining step in the disassembly process involves the initial attack of a β -CD molecule on a DNA-bound porphyrin, and not the formation of higher order complexes.

The form of the differential rate law that leads to eq 5 is (deceptively) simple:

$$-d[P]/dt = k_{\text{obs}}[P] \quad (6)$$

where $[P]$ is the concentration of porphyrin bound to DNA at time t ; i.e., the concentration of porphyrin not yet complexed by β -CD. Unlike more conventional rate laws, the rate constant, k_{obs} , has a time dependence which we have modeled as $k_{\text{obs}} = k_f t^{n+1}$. In this form, k_f is time-independent and has units of s^{-1} . As might be expected, k_{obs} (and therefore k_f) shows a dependence on $[\beta$ -CD], ($[\beta$ -CD]₀ \gg $[P]$ ₀). However, the state of the system (e.g., aggregate size, distribution, and fractal dimension) and therefore its reactivity may depend on porphyrin and DNA concentrations as well.¹¹ For poly(dG-dC)₂, no clear-cut dependence is seen over the conditions of our experiments (Figure 7a), although k_f may increase modestly with $[t$ -H₂P_{agg}]. For ct DNA, the measured rate constant at a constant β -CD concentration is somewhat more sensitive to starting conditions, increasing with porphyrin concentration and decreasing with ct DNA concentration.

Integrated rate laws having a stretched exponential time dependence, found here to be useful for fitting the data, are not without precedence in chemical kinetics. In 1939, Avrami proposed an equation of this form for describing the kinetics of polymer crystallization.²⁴ In his analysis, the exponent n was taken as a measure of both “seed-formation” dynamics and the dimension of the polymer, which was expected at the time to be integral. However, chiral aggregates of porphyrins on a DNA surface are of fractal dimension; light scattering measurements provide an estimate, $d_f \sim 1.9$ under the conditions of these experiments.¹¹ A general treatment for *aggregation* in a fractal space provided by Leyvraz leads to the conclusions that (i) the size of the aggregate scales as a power law of time (as described earlier) and (ii) the concentration of monomers decreases with a stretched exponential time dependence.¹⁴ Finally, an equation of this same form can be obtained from the nonconventional autocatalytic model proposed by us and described in the Introduction if “seed formation” is replaced as the rate-determining step by the binding of monomer units to a growing assembly; i.e., $m = 1$ in eq 1.¹⁶

In the present study on the *deaggregation* of a fractal array, a stretched exponential form of the experimental rate law proves effective at fitting the data. The analyses lead to $n > 0$, which implies that the DNA-bound porphyrin system becomes increasingly reactive with time. Thus, we consider the degradation of the porphyrin assembly by β -CD to be an autocatalytic process

in which the system becomes activated by the kinetic events. What is the basis of this kinetic activation?

The reaction rate constant, k_f , was determined as a function of β -CD concentration using three detection modes (Figure 8), and a linear dependence on $[\beta$ -CD] is observed for each set of experiments. However, whereas the kinetic results are nearly identical for circular dichroism and RLS detection, the extinction kinetics are significantly slower. Circular dichroism and RLS signals are both highly sensitive to aggregate size whereas absorbance (which is the major contributor to the extinction signal) depends primarily on concentration of aggregated porphyrins and less sensitively on the size of the array for aggregates larger than ~ 20 units.²⁵ Our results indicate that the second-order rate constant ($= k_f/[\beta$ -CD]) is roughly half as large when the concentration of porphyrins in aggregates is monitored than when the size of the aggregate is detected, for both poly(dG-dC)₂ and ct DNA templates.

The observation that the concentration of aggregated porphyrin units disappears more slowly than aggregate size has mechanistic implications for the mode(s) of β -CD attack on the aggregate and the source of the catalysis. The issue resolved by these results relates to the question, do β -CD molecules react with t -H₂P_{agg} at the ends of the aggregate only, with porphyrins anywhere in the aggregate, or only with the equilibrium concentration of free monomer? Dilution experiments allow us to exclude the last of these. If β -CD were simply a passive scavenger, its presence would not enhance the rate of deaggregation, only the extent. The dependence of the rate on the spectroscopic technique used to monitor the reaction allows us to rule out *end-only* attack of the aggregates. If this were the case, the concentration of aggregated monomers would decrease at precisely the same rate as the average aggregate size. On the other hand, attack at an interior site removes a t -H₂P_{agg} unit from the aggregate one molecule at a time, but severs the electronic coupling of the assembly, thereby reducing average aggregate size by a greater factor. The experimental rate would therefore be expected to be faster for RLS and circular dichroism detection than for absorbance, as observed. Furthermore, each time an interior porphyrin is removed, two new ends are created (ignoring penultimate porphyrins and annealing through assembly translocation). If ends are more reactive than interior molecules, the apparent rate constant for the transfer of porphyrins from the DNA surface would increase with time, as has been found experimentally.

These insights concerning the mechanism (autocatalysis, attack at interior sites as well as ends) suggest a strategy for modeling the process of aggregate degradation. We find that to achieve a satisfactory fit with the data requires a minimum of four kinetic parameters, one for β -CD attack at each of four different types of porphyrin sites. The model described below is incomplete in that it considers the array as a linear aggregate and thereby ignores branch points associated with a fractal array, it does not consider a dependence on the exact position of a porphyrin in the array or annealing, and it assumes the aggregates are always very large. As a consequence, the model becomes unrealistic near the end of the degradation process, and some 85–90% of the extinction change was selected for analysis. Despite its limitations, the modeling results are

(22) Manning, G. S. *Q. Rev. Biophys.* **1978**, *11*, 179–246.

(23) Pasternack, R. F.; Garrity, P.; Ehrlich, B.; Davis, C. B.; Gibbs, E. J.; Orloff, G.; Giartosio, A.; Turano, C. *Nucleic Acids Res.* **1986**, *14*, 5919–5931.

(24) Avrami, M. *J. Chem. Phys.* **1939**, *7*, 1103–1112

(25) Parkash, J.; Robblee, J. H.; Agnew, J.; Gibbs, E.; Collings, P.; Pasternack, R. F.; de Paula, J. C. *Biophys. J.* **1998**, *74*, 2089–2099.

included here to illustrate that the conclusions arising from a nonconventional approach are consistent and adequate to account for the general experimental kinetic profile.

The four types of porphyrins considered in the more conventional analysis are as follows: end (Y), penultimate (W), interior (Z), and isolated (I) units. Differential rate laws are written as

$$\begin{aligned} Y' &= 2k_Z[Z] \\ Z' &= -5k_Z[Z] - k_Y[Y] - 2k_W[W] \\ I' &= -k_I[I] + k_W[W] \\ W' &= 2k_Z[Z] \end{aligned} \quad (7)$$

Equations 7 embody the approximations and assumptions described earlier. Thus, each time an end porphyrin is removed, a penultimate unit becomes an end and an interior unit becomes a penultimate. When a penultimate porphyrin is removed by a β -CD molecule, the end molecule becomes isolated and two interior porphyrins are converted, one to an end and the other to a penultimate. Finally, when an interior porphyrin is removed, two new ends and two penultimates form. These considerations, which account for the numerical constants used in eqs 7, require the aggregates to be long to be valid. Numerical integrations were carried out for the system of equations using *Scientist*, a software package provided by Micromath Scientific Software (Salt Lake City, UT), and the best fit, shown in Figure 9, was obtained with rate constants, $k_Y = 0.46 \text{ s}^{-1}$, $k_W = 0.15 \text{ s}^{-1}$, $k_Z = 0.043 \text{ s}^{-1}$, and $k_I = 0.0037 \text{ s}^{-1}$. As anticipated by the autocatalytic model presented above, $k_Y, k_W > k_Z$. The small value of k_I suggests that an isolated porphyrin unit rapidly intercalates,^{5,26} leading to slow removal by β -CD.

In summary, an analysis of porphyrin-array disassembly kinetics, in which time-dependent rate constants are incorporated, leads to a precise fit of the data. Whereas this approach provides only a "global overview" of the system's kinetic behavior and yields mechanistic information indirectly, it benefits from its simplicity and its success in fitting the data with a small number of parameters. Such an approach permits

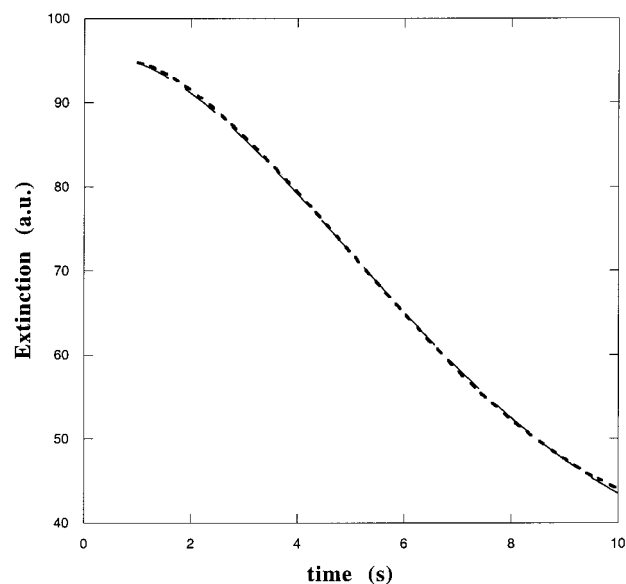


Figure 9. Results of numerical integration using the system of eqs 7. The kinetic data (---) are a portion of the data shown in Figure 6 (see text). The model used for the analysis is successful at fitting this part of the data profile (—). At longer times, large deviations between the data and the model are apparent. The best fit was obtained with second-order rate constants (after division by $[\beta\text{-CD}]$) for attack at ends and penultimate sites as 11 and $3.6 \text{ M}^{-1} \text{ s}^{-1}$, respectively. The rate constant for an interior position is $1.1 \text{ M}^{-1} \text{ s}^{-1}$, and the rate constant for attack by β -CD of an isolated porphyrin is $0.92 \text{ M}^{-1} \text{ s}^{-1}$.

direct comparison of kinetic constants for similar systems, allowing evaluation of the impact of systematic component and mode of detection variation on the disassembly (or assembly¹¹) processes. The availability of this information can, as in the present case, lead to a mechanistic argument (expressed in terms of elementary steps) which when evaluated by conventional methods provides rate constants for the individual reactions.

Acknowledgment. This work was supported by the National Science Foundation through Grant CHE-9900403, the National Institutes of Health (Grant AG 19302-01), the Howard Hughes Medical Institute, and Swarthmore College through a Lang Faculty Fellowship. We gratefully acknowledge useful conversations with Professors Julio dePaula of Haverford College and Peter Collings of Swarthmore College.

(26) Pasternack, R. F.; Gibbs, E. J.; Villafranca, J. J. *Biochemistry* **1983**, *22*, 5409–5417.